ISSN: 3064-9846
Review Article
Science Set Journal of Economics Research

The Method of Reducing Distortions in the Radar Image of the Earth's Surface Caused by Changes in the Course of The Movement of the Synthetic Aperture Radar

Andrei Sidorov[1*], Svetlana Svistova[2], & Tatiana Nikitina[3]

[1]*Alexandru Ioan Cuza University of Iasi, Faculty of Economics and Business Administration Bulevardul Carol I nr. 22, Iași 700505, Iasi, Romania*
[2]*RTU MIREA – Russian Technological University, Department of higher mathematics No. 1, Institute of Artificial Intelligence, 78 Vernadsky Avenue, Moscow, 119454, Russia*
[3]*RTU MIREA – Russian Technological University, Department of Higher and Applied Mathematics, M.V. Lomonosov Institute of Fine Chemical Technologies, 86 Vernadsky Avenue, Moscow, 119454, Russia*

[*]Corresponding author: Andrei Sidorov, Alexandru Ioan Cuza University of Iasi, Faculty of Economics and Business Administration Bulevardul Carol I nr. 22, Iași 700505, Iasi, Romania.

Submitted: 03 June 2025 **Accepted:** 11 June 2025 **Published:** 16 June 2025

https://doi.org/10.63620/MKJAEES.2025.

Citation: *Sidorov, A., & Svistova, S., Nikitina, T. (2025). The Method of Reducing Distortions in the Radar Im age of the Earth's Surface Caused by Changes in the Course of The Movement of the Synthetic Aperture Radar. Sci Set J of Economics Res, 4(3), 01-06.*

Abstract

The article addresses distortions in synthetic aperture radar (SAR) images caused by the non-linear motion of the radar platform. Such motion, often due to navigation errors, environmental factors, or maneuvering, introduces Doppler frequency components into the received signal. These distortions lead to reduced image intensity and multiple displaced replicas of objects along the flight path. Analytical and simulation results show intensity can drop to 45% of the undistorted value, with object replicas appearing at regular intervals related to Doppler shift and system parameters. To counter this, the paper proposes a method that estimates Doppler components and applies a time-dependent phase correction via numerical integration. This correction is implemented before standard SAR processing and does not require precise knowledge of the platform's trajectory. Simulations show that with up to 20% estimation error, image intensity is restored to 85% and artifacts are suppressed. The method is efficient, practical, and compatible with existing SAR systems.

Keywords: Doppler Frequency Estimation, Phase Error Correction, Non-linear Platform Motion, SAR Image Reconstruction, Remote Sensing Accuracy

Introduction

Synthetic Aperture Radars (SAR), commonly mounted on aircraft and used to survey the Earth's surface, achieve ultra-high azimuth resolution through antenna movement, memory of received signals, and their coherent processing. This technique is equivalent to using an antenna array with an aperture size comparable to the distance traveled. High range resolution is made possible by the use of wideband signals, and SAR images are of comparable quality to aerial photography, with the added advantage that they are unaffected by time of day or weather conditions and can be obtained over long ranges [1, 2]. The aperture synthesis algorithm, based on matched filtering of signals reflected from the surface, assumes a straight and uniform path for the SAR. However, deviations from this path lead to distortions in the resulting image, affecting both resolution and accuracy.

Such distortions, caused by non-linear motion, are a significant challenge in SAR applications. Several motion compensation

methods have been proposed to address this issue. Feng et al. (2023) introduced a method based on subaperture processing, assuming nearly constant velocity within segments of radar data to correct motion errors and improve imaging precision [3]. Similarly, Zhang et al. (2022) developed a nonlinear chirp scaling algorithm that compensates for spatial variance due to non-linear motion by applying corrections to smaller image blocks, improving both efficiency and resolution [4]. Han et al. (2022) proposed a method that maximizes the sharpness of dominant scatterers within sub-images, correcting errors in both the range and azimuth dimensions, particularly for high-resolution wide-swath (HRWS) SAR systems [5]. For circular SAR configurations, Li et al. (2024) introduced an algorithm that uses radial acceleration data to correct phase errors, even without detailed inertial navigation system data [6]. Xie et al. (2014) adapted the nonlinear chirp scaling algorithm to correct distortions caused by curvilinear flight paths, improving geometric accuracy without the need for interpolation [7].

Motion compensation in SAR is crucial across various platforms, including satellites, drones, and autonomous vehicles, due to its role in maintaining image accuracy and resolution. For satellite-based SAR systems, especially low Earth orbit (LEO) satellites, rapid orbital motions can induce significant distortions that affect image quality [8]. Similarly, UAVs and drones, used in applications such as environmental monitoring and disaster response, rely on precise motion compensation to correct distortions caused by non-linear flight paths [9, 10]. In military surveillance and reconnaissance, SAR systems on aerial platforms require motion compensation to ensure reliable, high-resolution images, especially in complex terrains [11]. The importance of this technology also extends to space exploration, where SAR is used to map planetary surfaces, such as the Moon and Mars, and motion correction is essential for accurate terrain analysis [12]. In summary, motion compensation enhances the capabilities of SAR across high-stakes applications, including Earth observation, space exploration, and disaster management [13].

The aim of this article is to analyze the distortions in Earth's surface images caused by non-linear SAR motion and propose a method to reduce these distortions, thereby improving the reliability and accuracy of SAR-based Earth observation.

Analysis and Correction of Image Distortions in Synthetic Aperture Radar Due to Non-Linear Platform Motion

Let us assume that the carrier of the synthetic aperture radar (SAR) system, such as an airplane or helicopter, moves in a straight line and at a constant speed V along the designated path (DP), which coincides with the x -axis in Figure 1. The radar antenna, mounted along the fuselage, forms a beam with an angular width θ in azimuth, directed perpendicular to the DP. During the movement, the carrier continuously transmits and receives reflected signals from the underlying surface.

A point target located at point C (Figure 1) is observed by the synthetic aperture radar (SAR) system within the path segment [-L/2;L/2]. Beyond this range, the target exits the antenna's coverage area, and its reflected signal does not reach the radar.

When the synthetic aperture radar (SAR) system is at the point x(t), it transmits a signal of the form: U_0 e^(j2πf_0 t) , where (U_0 - the signal amplitude, f_0 - the carrier frequency, and t – time).The signal reflected from the point target is received by the SAR with a delay t_z=2R(t)⁄c, where (R(t) - the current distance from the SAR to the target, and c - the speed of radio wave propagation). The amplitude of the received signal decreases to U due to wave propagation and attenuation of the reflected signal:

$$u_{rec}(t) = Ue^{j2\pi f_0(t-2R(t)/c)} \quad (1)$$

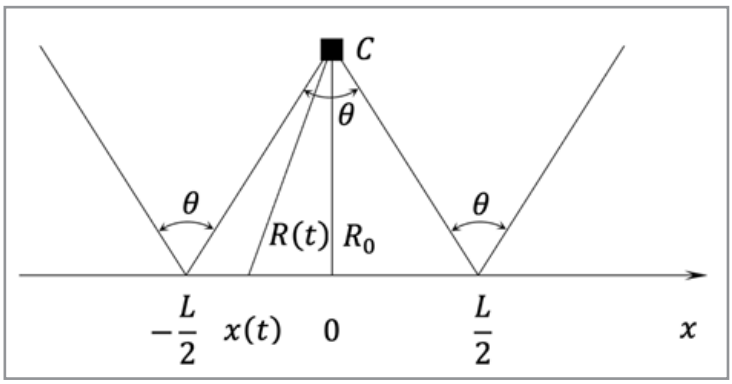

Figure 1: Detection and Registration of a Point Target Using SAR.

When the synthetic aperture radar (SAR) system moves along the designated path (DP), its coordinate changes according to the law: x(t)=Vt , where (V-the carrier speed, and t – time). The distance to the point target R(t) also changes over time and is determined by the following expression:

$$R(t) = \sqrt{R_0^2 + x^2(t)} \approx R_0\left(1 + \frac{1}{2}\left(\frac{x(t)}{R_0}\right)^2\right) = R_0 + \frac{(Vt)^2}{2R_0} \quad (2)$$

Where R_0 is the distance from the point target to the DP, with the condition x(t)⁄(R01). Considering relations (1) and (2), the signal received by the SAR will be as follows:

$$u_{rec}(t) = \begin{cases} Ue^{-j2\pi((Vt)^2/(\lambda R_0)+2R_0/\lambda)}e^{j2\pi f_0 t}, & |t| \le T/2, \\ 0, & |t| > T/2, \end{cases} \quad (3)$$

Where:
λ – the wavelength of the emitted signal
T – the aperture synthesis time, which corresponds to the interval during which the carrier, moving along the path segment [-L/2;L/2], observes the point target.
The value of the aperture synthesis interval is determined by the following expression:

$$T = \frac{L}{V} = \frac{R_0\theta}{V} = \frac{R_0\lambda}{aV} \quad (4)$$

The value of the aperture synthesis interval is calculated using the following expression, which incorporates the well-known relationship for the beam width θ=λ⁄a (where a - the horizontal size of the radar antenna), as well as the estimate LR0 θ, obtained for small values of the beam width θ1.

From relations (3) and (4), the expression for the complex envelope of the signal from the point target on the synthesis interval |t| (≤T)⁄2 follows, where φ_0=(4πR_0)⁄λ is the constant phase:

$$u_{env}(t) = u_{rec}(t)e^{-j2\pi f_0 t} = Ue^{-j\left((\pi(2\lambda R_0)/a^2)(t/T)^2+\varphi_0\right)} \quad (5)$$

From expression (5), it follows that the complex envelope of the signal from the point target is a signal with linear frequency modulation (LFM) with decreasing frequency and a bandwidth B=ΔfT=(2λR_0)⁄a^2 , where Δf - the frequency deviation, and T is the duration of the synthesis interval.

The aperture synthesis algorithm includes the calculation of the filter response, tuned to the signal from the point target (expression (5)) to the complex envelope of the input signal of the SAR (Kondratenkov et al., 1983, p. 92).

The impulse response h(t) of the matched filter for the SAR is determined by the following formula, where k - a dimensional constant:

$$h(t) = ke^{j\pi\frac{2\lambda R_0}{a^2}\left(\frac{t}{T}\right)^2}, \quad |t/T| \le 1/2 \quad (6)$$

The signal from the point target, shifted by the Doppler frequency f_d (the case of signal shift by Doppler frequency will be considered later, for straight-line motion of the SAR f_d=0), at the output of the synthesis algorithm will be:

$$u_{out}(\tau, f_d) = \int_{-\infty}^{\infty} u_{env}(t)e^{j2\pi f_d t}h(t-\tau)dt =$$

$$= U_{max}\,e^{j(\pi f_d \tau-\varphi_0)}\frac{\sin\left(\pi\left(\frac{\lambda R_0 f_d}{aV}-\frac{2V\tau}{a}\right)\left(1-\left|\frac{\tau}{T}\right|\right)\right)}{\pi\left(\frac{\lambda R_0 f_d}{aV}-\frac{2V\tau}{a}\right)}, for\ |\tau| \le T \quad (7)$$

Where U_{max}= UkT.

The derivation of formula (7) for the LFM signal at the output of the matched filter is conducted in the same manner as in, with the difference that the frequency of the considered LFM signal decreases [14].

Figure 2 shows the signal u_out (τ,0)from the point target after processing by the synthesis algorithm with f_d=0 in the main lobe region.

The duration of the point target signal at the input of the synthesis algorithm was T, and at the output it became a/2V (it is assumed that the signal duration is equal to the abscissa of the first zero), i.e., it decreased by a factor of 2VT/a=(2λR_0)/a^2 =B, the bandwidth [15].

The resolution of the SAR along the line of motion is defined as the minimum distance δ_x=min⁡d between two-point targets at which the SAR responses to them are observed separately. The time offset between such responses is t_zmin=a⁄2V. Since during the time t_zmin, the SAR travels a distance of Vt_zmin, the resolution along the line of motion is δ_x=Vt_zmin (=a)⁄2, i.e., half the horizontal size of the antenna, and it does not depend on the distance to the target, the wavelength, or the velocity of the SAR carrier [16].

A radar image (RI) of an object is defined as the magnitude of the signal at the output of the aperture synthesis algorithm. The RI of a point target will be J(τ)=|u_out (τ,f_d)|.

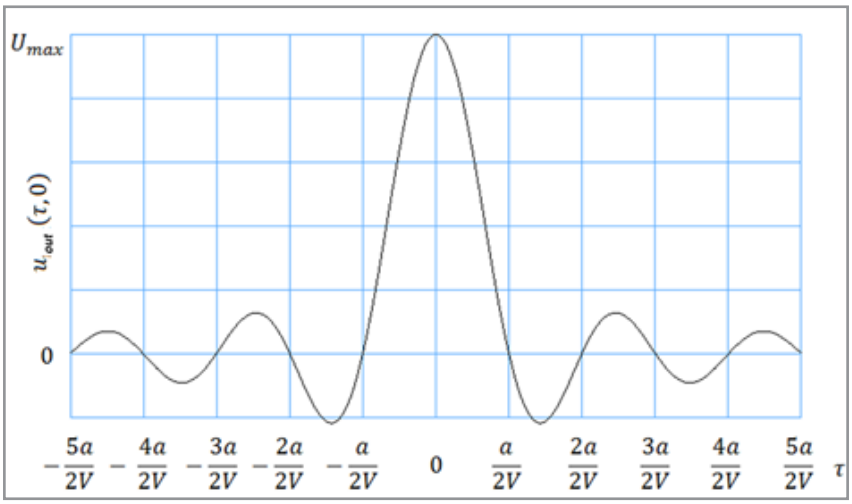

Figure 2: The Signal from the Point Target After Aperture Synthesis

Due to the influence of the atmosphere (wind, turbulence) and the control system (pilot or autopilot), the actual trajectory of the SAR carrier takes the form of a sinusoid "enveloping" the straight line of the designated path (LDP), as shown in Figure 3. This trajectory can be approximated by a broken line, identifying three characteristic types of segments: 1 – a straight segment crossing the LDP while approaching the object; 2 – a straight segment parallel to the LDP; 3 – a straight segment crossing the LDP while moving away from the object. The carrier's trajectory can be represented as an alternating sequence of segments 1, 2, 3, 2, 1, 2, 3, 2, …

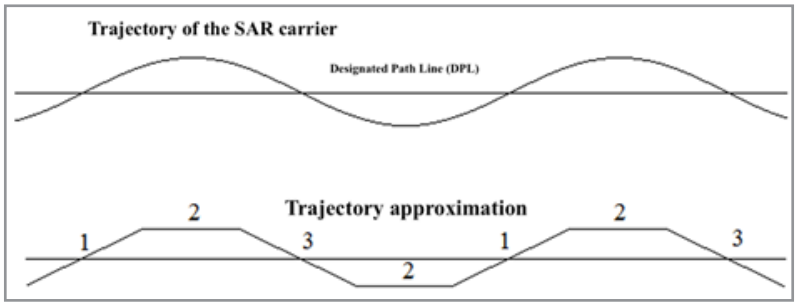

Figure 3: Trajectory of the SAR Carrier's Motion and its Approximation.

The signal from the point target corresponding to the carrier's motion along segments of type 2 will have linear frequency modulation (LFM). Meanwhile, the signals associated with the carrier's motion along segments of types 1 and 3 will also have LFM, but with Doppler frequency shifts: positive on segments of type 1 when approaching the target, and negative on segments of type 3 when moving away from the target.

According to the theory of matched processing of LFM signals and the analysis of formula (7), if an LFM signal with a decreasing frequency, shifted by a positive Doppler frequency, is input into the matched filter, the filter response will be delayed in time compared to the response to an LFM signal without frequency shift. In the case of a signal with a negative Doppler frequency shift, the filter response will occur earlier. From formula (7), it follows that the amount of time shift τ_sm of the signal maximum due to the Doppler effect is: (τ_sm=λR_0 f_д)/((2V^2)) where λ - the wavelength, R_0 - the distance from the object to the DPL, f_d- the Doppler frequency, and V - the speed of the carrier.

If the SAR trajectory contains segments of types 1, 2, and 3 within the synthetic aperture interval, the resulting radar image (RI) of the point object will contain three images located along the line of path: the first image corresponds to type 3 segments with the SAR moving away from the object and the LFM signal shifted to a negative Doppler frequency (leading image); the second image corresponds to type 2 segments without frequency shift of the LFM signal (image "in its place" – without delay or advance); the third image corresponds to type 1 segments with the LFM signal shifted to a positive Doppler frequency (lagging image). The magnitude of the image shift d_sm -equal to d_sm=(τ_sm V=λR_0 f_d)/((2V)).

If the synthetic aperture interval contains two segments, the radar image (RI) of the point object will contain two images: a leading image and an "in-place" image for segments 3 and 2, and a lagging image and an "in-place" image for segments 1 and 2. When the synthetic aperture interval contains only one segment, the RI of the point object will have a single image: "in-place" for segment 2, leading or lagging for segments 3 and 1, respectively.

The RI of the Earth's surface is a set of images of point objects that differ in intensity. Distortion of the image of the Earth's surface and the objects on it, caused by the non-linear motion of the SAR carrier, is manifested in the multiplication and displacement of images of point and extended objects that are not aligned parallel to the reference path. As a result, instead of one image, for example of a power line pole or road, multiple images may be obtained — three, two, or one, but displaced.

The provided estimates of the effect of non-linear SAR motion on the image of a point object are confirmed by computer modeling. A model using the synthetic aperture algorithm allows generation of the RI of a point object for various SAR motion trajectories.

Figure 4 shows the RI of a point object corresponding to SAR motion along a straight segment of type 2. This RI matches the magnitude of the point object signal at the output of the synthetic aperture algorithm (Figure 2) in the appropriate scale. As seen in Figure 4, the RI of the point object is located at the point with coordinate x=0, just like the object itself in Figure 1.

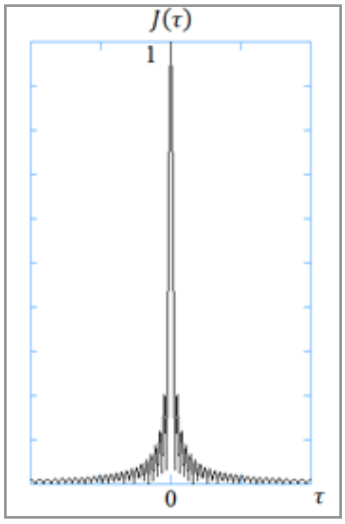

Figure 4: Undistorted Radar Image (RI) of a Point Object During SAR Motion Along a Segment of type 2.

Figure 5 shows the radar image (RI) of a point object corresponding to SAR motion along segments of types 1, 2, and 3. The figure shows that the RI intensity decreases to 0.45 of the undistorted level, and the image of the point object splits into three separate images. Thus, the simulation confirmed that linear SAR motion does not distort the RI, while nonlinear motion causes image distortions: for a SAR trajectory containing segments of types 1, 2, and 3, the image triples, and its intensity decreases to 0.45 compared to the undistorted RI.

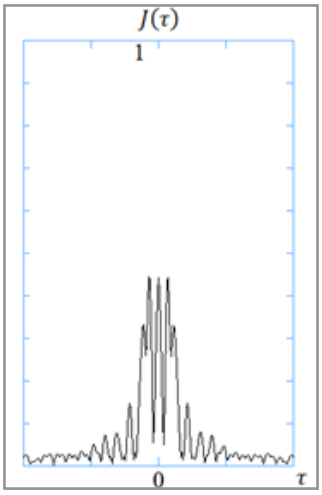

Figure 5: Radar Image (RI) of a Point Object During SAR Motion Along Segments of Types 1, 2, and 3.

A method is proposed to reduce surface image distortions caused by non-linear motion of the SAR platform. The method is based on estimating the Doppler frequency f^_d (t) of the signal received by the SAR. The obtained estimate of the Doppler frequency is then used to integrate and obtain an estimate of the phase φ^(t) of the received signal:

$$\hat{\varphi}(t) = 2\pi \int_{-T/2}^{t} \hat{f}_d(\tau)\, d\tau \qquad (8)$$

To eliminate the distortion of the RLI, a phase correction is introduced into the received signal s(t)·e^(-jφ^(t)). The signal with the phase correction is then processed by the aperture synthesis algorithm. This significantly reduces the image distortions, which is confirmed by the SAR simulation results presented in Figure 6. This figure shows the RLI of a point object during the SAR movement along sections of type 1, 2, and 3 with compensation for the phase roll-off (8) in the signal, for the case of Doppler frequency estimation with an error of 20%. Comparing the quality of the RLI shown in Figures 4 and 6 demonstrates that compensating for the Doppler frequency significantly improves the RLI: the effect of image tripling is eliminated, and its intensity increases from 0.45 to 0.85 of the undistorted RLI.

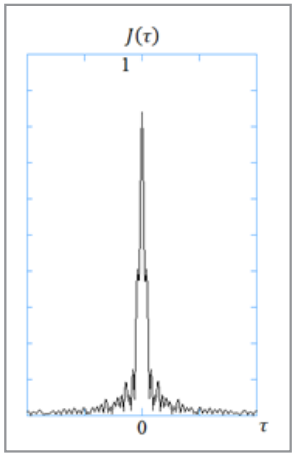

Figure 6: Radar Image (RLI) of a Point Object when the Synthetic Aperture Radar (SAR) Moves Along Sections of type 1, 2, and 3 with Compensation for the Doppler Frequency Measured with a 20% Error.

It should be noted that obtaining an estimate of the Doppler frequency with acceptable accuracy for compensating the nonlinear motion of the SAR is a challenging task, the solution to which for various models of the underlying terrain is a subject of study.

Conclusions

The nonlinear motion of the SAR introduces one or more Doppler frequencies into the received signal. It is shown analytically and confirmed by modeling that the presence of Doppler frequencies in the signal leads to a decrease in the intensity of radar images to values of 0.45 of the intensity of undistorted images and to the multiplication of images with displacement along the path. The size of the image displacement caused by the Doppler frequency shift f_d, is equal to (λR_0 f_d)/((2V)).

A method for reducing image distortions of the Earth's surface is proposed, which involves estimating the Doppler frequency of the signal received by the SAR. The phase φ(t) is obtained from the estimate by integration and is introduced as a correction to the received signal, which is then input to the aperture synthesis algorithm. This method significantly improves the quality of the radar images: the multiplication of images and their displacement are eliminated. When the Doppler frequency is estimated with a 20% error, the intensity of the recovered radar image is 0.85 of the undistorted value.

References

1. Kondratenkov, G. S., & Frolov A. Yu. (2005). Radiovision. Radar Remote Sensing Systems of the Earth, Radiotekhnika Publ., Moscow, 368.
2. Kondratenkov, G. S., Potehin, V. A., Reutov, A. P., & Feoktistov, Yu. A. (1983). Earth Observation Radar Stations, Ed. by G.S. Kondratenkov, Radio i Svyaz Publ., Moscow, 272.
3. Feng, G., Liu, L., Luo, J., Jiang, L., Xu, Z., & Lin, J., (2023). A Combined Motion Compensation Method for Long Synthetic Aperture Radar Based on Subaperture Processing, Journal of Marine Science and Engineering, 13(2), 355.
4. Zhang, J., Zhang, D., Huang, Y., & Ma, M. (2022). Sub-Image Nonlinear Chirp Scaling for Two-Dimensional Spatial Variance Correction, Journal of Radars, 11(2), 215-226.
5. Han, G., Li, D., Liu, L., Zhang, H., & Li, H., (2022). A Motion Error Compensation Method Based on Sub-Image Reconstruction for HRWS SAR, Remote Sensing, 14(4), 1033.
6. Li, D., Zhang, H., Han, G., Zhang, Y., & Yang, G. (2024). Motion Compensation Algorithm Using Radial Acceleration Data for Circular SAR Imaging, Remote Sensing, 16(4), 623.
7. Xie, Y., Zhang, Q., Wu, B., & Li, S., (2014). A Modified Nonlinear Chirp Scaling Algorithm for Curvilinear Trajectory SAR, Journal of Central South University, 21(5), 1832-1840.
8. Kalluri, S., & Reddy, D. (2021). Satellite-based SAR systems for Earth observation and motion compensation techniques, Remote Sensing Journal
9. Gao, Y., & Zhang, Z. (2019). UAV-mounted SAR for environmental monitoring and agricultural applications, IEEE Transactions on Geoscience and Remote Sensing.
10. Lin, Z., & Wu, X. (2020). Motion compensation for SAR systems on drones: Application to disaster response, Journal of Field Robotics.
11. Huang, R., & Lee, J. (2019). SAR systems for military reconnaissance on UAVs: Motion compensation methods, Journal of Aerospace and Defense Technology.
12. Lemoine, G., & Therrien, P. (2020). SAR-based planetary mapping for space exploration missions, International Journal of Space Science.
13. Bürgmann, P. (2021). Use of SAR for post-disaster monitoring and emergency response, Natural Hazards and Earth System Sciences.
14. Bernfeld, M., & Cook, C. (1971). Radar Signals, Transl. from English, Ed. by V.S. Kelzon, Sov. Radio Publ., Moscow, 568.
15. Antipov, V. N., Goryainov, V. T., & Kulin, A. N. (1988). Radar Stations with Digital Aperture Synthesis, Ed. by V.T. Goryainov, Radio i Svyaz Publ., Moscow, 304.
16. Kulin, A. N., & Goryainov, V. T. (1988). Radar Stations with Digital Aperture Synthesis, Ed. by V.T. Goryainov, Radio i Svyaz Publ., Moscow, 304.